

# MICROPHONICS AND LORENTZ TRANSFER FUNCTION MEASUREMENTS ON THE SNS CRYOMODULES \*

J. R. Delayen, G. K. Davis, Jefferson Lab, 12000 Jefferson Ave., Newport News, VA 23606, USA

## Abstract

As part of the acceptance tests, we have performed a number of measurements of microphonics levels and frequency spectra on the SNS cryomodules. These measurements are particularly important since those cryomodules may be used in the high-energy section of the RIA driver, a low-current CW accelerator. Measurements of the complete transfer functions between rf field modulation and cavity resonant frequency have also been performed.

## BACKGROUND MICROPHONICS PROBABILITY DENSITY FUNCTION

As part of SNS production cryomodule acceptance testing [1], a microphonics histogram was obtained for each cavity. Data sets as large as 400,000 samples at up to 500 samples/sec were obtained. Representative data are shown in Figure 1 and Figure 2. The cavity frequency detuning was measured with a Cavity Resonance Monitor [2], and was bandpass filtered between 1 Hz and 1 KHz to remove the high frequency noise and the slow frequency drifts. Some assemblies showed dramatic time variation of the microphonics levels, presumably due to refrigeration LHe fluid dynamics. Peak transient microphonics levels resulting in up to 50 Hz cavity detuning have been observed.

All assemblies easily meet the SNS specification for  $6\sigma < 100$  Hz. The RIA application requires  $\sigma < 3.5$  Hz. Some combination of passive and active controls might be required for these cryomodules to be used in RIA.

## MICROPHONICS SPECTRUM

The microphonics spectrum was measured concurrently with each histogram. Some spectral peaks correspond to the cryomodule assembly mechanical resonances being excited by broadband background vibrational energy, (compare Fig 3 with Fig 7, and Fig 4 with Fig 8) while others result from peaks in the background vibration spectrum itself (e.g. 60 Hz harmonics).

Note the dominant peak at 8 Hz for assembly M03, cavity 1. This peak caused the bimodal shape shown in the histogram (Fig. 2). Most tests resulted in a gaussian distribution, as shown for M02, cavity 3 (Fig. 1).

The majority of the energy is at lower frequencies, where electronic feedback vibration control is generally easier to implement. The differences in the spectra imply that any microphonics feedback control scheme will have to be flexible and adaptable, perhaps even customized for each cavity.

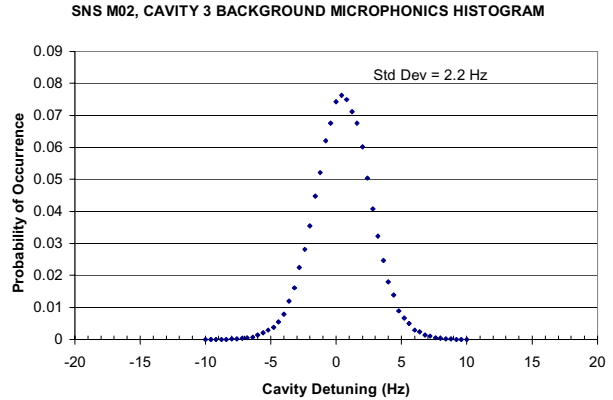


Figure 1: Background Microphonics PDF, gaussian

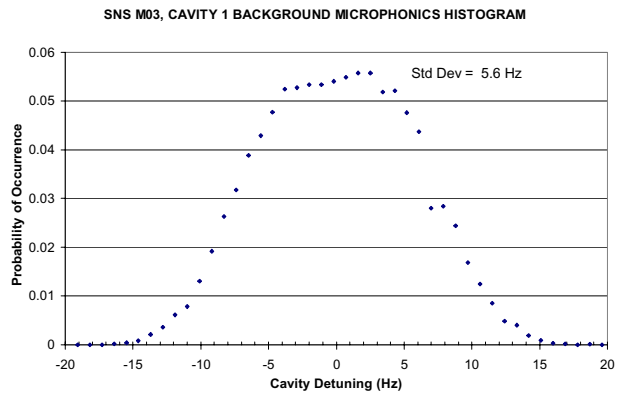


Figure 2: Background Microphonics PDF, bimodal

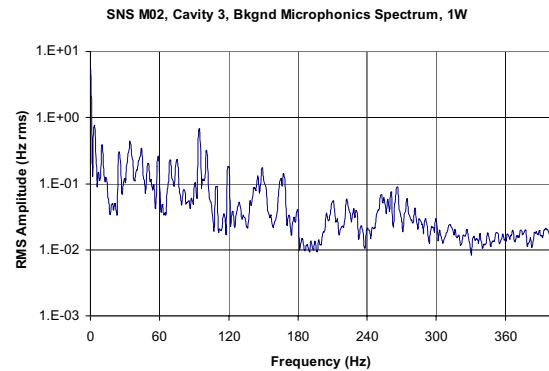


Figure 3: Typical background microphonics spectrum

\* \*Work supported by the U.S. Department of Energy, contract DE-AC05-84ER401050

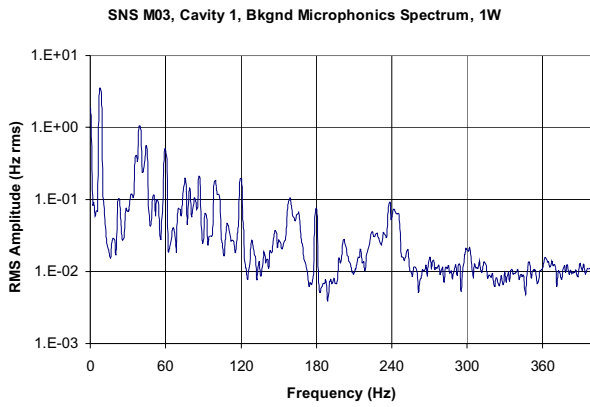


Figure 4: Background microphonics spectra, 8Hz dominant

## LORENTZ TRANSFER FUNCTION MEASUREMENT

The transfer function between the RF field amplitude and the resulting cavity detuning was measured in each cavity of the first four SNS medium  $\beta$  cryomodules.

The static Lorentz coefficient is determined by establishing a 5 MV/m accelerating gradient, and then measuring the cavity detuning that results from a 10% amplitude modulation using a 0.2 Hz square wave. This rate is slow enough to avoid mechanical resonances, and fast enough to eliminate slow drift due to LHe pressure variations. The equipment block diagram is shown in Fig. 5. The output signal from the cavity resonance monitor is low-pass filtered at 1 Hz to remove high frequency microphonics. A typical measurement result is shown in Fig. 6.

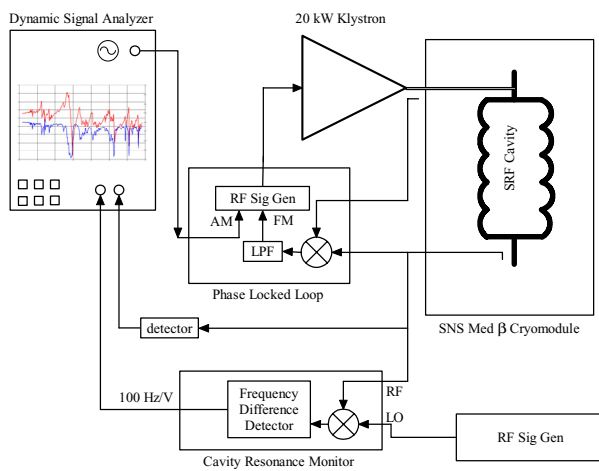


Figure 5: Lorentz transfer function measurement block diagram.

Once the static coefficient has been established, the dynamic variation at higher frequencies is measured. An HP35670A Dynamic Signal Analyzer is used to generate a swept sinusoid that is used to amplitude modulate the LLRF drive. The average accelerating gradient of 5 MV/m is modulated by 10%. The signal analyzer computes the amplitude and phase response between the transmitted power (RF diode detector output, proportional to Eacc) and the cavity detuning (cavity resonance monitor output, low-pass filtered at 1 kHz to remove the slow drifts).

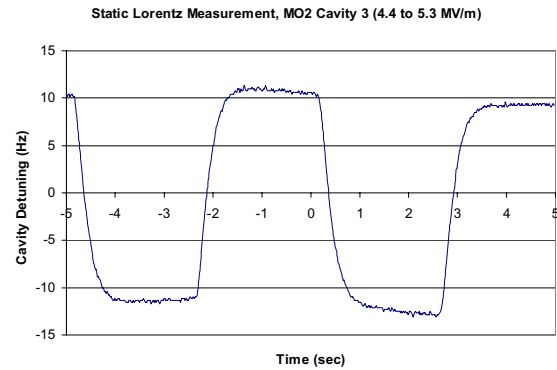


Figure 6: Static Lorentz measurement

Small, but significant differences between the transfer functions from cavity to cavity were observed (see Fig. 7 and Fig. 8). This data will be incorporated into the RIA and SNS LLRF modeling efforts, and eventually the respective LLRF control systems [3]. As shown in Fig. 9, further differences exist between the Lorentz transfer function and the piezo actuator transfer function for the same cavity [4]. In particular, the zeroes in the responses occur at slightly different frequencies; this was observed on several cavities. These differences further complicate electronic vibration control since the actuator is to be used to control the vibration.

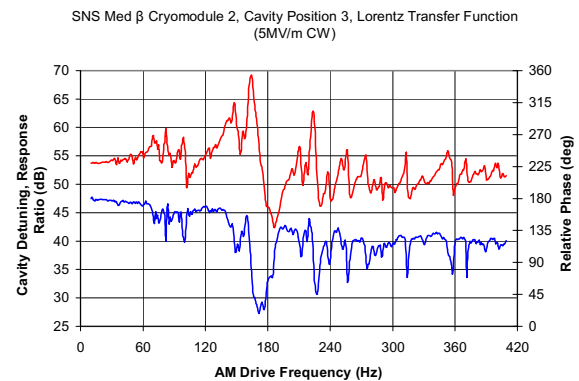


Figure 7: Dynamic Lorentz transfer function, position 3.

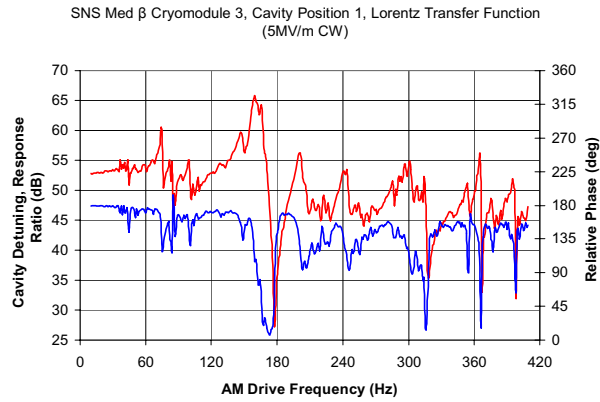


Figure 8: Dynamic Lorentz transfer function, position 1

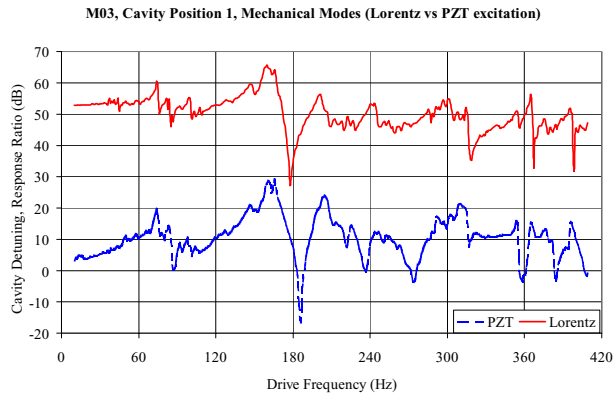


Figure 9: Dynamic Lorentz and PZT transfer functions

## REFERENCES

- [1] Jean Delayen, Ed Daly, Kirk Davis, Steve Smee, "Frequency Measurements on the Prototype SNS Medium-b Cryomodule Under Pulsed and CW Operation," JLab Tech Note 02-049.
- [2] G. Kirk Davis, Jean Delayen, Michael Drury, Thomas Hiatt, Curt Hovater, Thomas Powers, Joseph Preble, "Microphonics Testing of the CEBAF Upgrade 7-Cell Cavity," PAC 2001, Chicago, IL, 18-22 June 2001.
- [3] Alicia Hofler, Jean Delayen, Curt Hovater, Stefan Simrock, "RF System Modeling for the JLab 12 GeV Upgrade and RIA," these proceedings
- [4] J. R. Delayen, G. K. Davis, "Piezoelectric Tuner Compensation of Lorentz Detuning in Superconducting Cavities," these proceedings.